JOURNAL OF CATALYSIS 151, 253–265 (1995)

Transient Response of Propionaldehyde Formation during $CO/H_2/C_2H_4$ Reaction on Rh/SiO_2

Michael W. Balakos and Steven S. C. Chuang[1]

Department of Chemical Engineering, The University of Akron, Akron, Ohio 44325-3906

Received March 8, 1994; revised September 28, 1994

The transient response of propionaldehyde formation during ethylene hydroformylation over Rh/SiO_2 has been studied by transient isotopic methods combined with *in situ* infrared spectroscopy at 0.1–0.5 MPa and 503 K. The transient methods used in this study involved pulsing ^{13}CO into the CO feed flow and switching from CO to ^{13}CO flow. The $C_2H_5{}^{13}CHO$ response to the ^{13}CO step input was found to be equivalent to the integration of the $C_2H_5{}^{13}CHO$ response to the pulse input with respect to time. The pulse method allows the economical use of costly isotope to obtain the transient information that is commonly acquired from the step method. Analysis of the transient response reveals that the propionaldehyde may be formed via (i) the insertion of CO into adsorbed ethyl species to form the acyl intermediate, (ii) hydrogenation of the acyl intermediate to produce adsorbed propionaldehyde, and (iii) desorption of adsorbed propionaldehyde. Increasing the total reaction pressure (i.e., increasing all partial pressures in the same ratios) increases the rate constant for hydrogenation of the acyl intermediate which has been identified as the rate-determining step for propionaldehyde formation at 0.1 MPa. Increasing the pressure also increases the coverage, but decreases the residence time of intermediates leading to propionaldehyde. Steady-state rate mesurements show that increasing reaction pressure decreased the overall activation energy and increased both rate and selectivity for propionaldehyde. The increase in the rate constant for hydrogenation of acyl intermediate can be related to the decrease in the overall activation energy for propionaldehyde formation. Rate constant analysis of the propionaldehyde response shows that the rate constant for propionaldehyde formation exhibits a sharp single distribution. © 1995 Academic Press, Inc.

INTRODUCTION

The reaction of ethylene with syngas (CO/H_2) has been used as a probe reaction to study the activity of transition metal catalysts for C_{2+} oxygenate formation during the Fischer–Tropsch (F–T) synthesis (1–6). Catalysts that exhibit good C_{2+} oxygenate activity in the F–T synthesis also demonstrate high activity for the formation of propionaldehyde (C_3 oxygenate) in the $CO/H_2/C_2H_4$ reaction, also known as ethylene hydroformylation (7–10). The common activities for C_2 and C_3 oxygenate formation stem from CO insertion into an alkyl-metal bond of a surface intermediate being a common key step in both reactions (1–4). In the F–T reaction, C_2 oxygenates result from CO insertion into adsorbed CH_x intermediates that are formed from the dissociation of CO and subsequent hydrogenation (4, 11–15). C_3 oxygenates result from CO insertion into adsorbed C_2H_x intermediates produced from adsorbed ethylene in the heterogeneous hydroformylation reaction (1–5, 14). The parallel reaction step, i.e., the CO insertion step, between the two allows ethylene hydroformylation to be used as a probe to study CO insertion in the F–T synthesis without the complexities of the CO dissociation step.

The activity and the selectivity of a catalyst for CO insertion are a complex function of reaction conditions and catalyst composition. Increasing temperature results in low selectivity for oxygenate formation and high selectivity for hydrocarbon formation during the F–T and $CO/H_2/C_2H_4$ reactions (5, 16, 17). Increasing the total pressure (i.e., increasing all partial pressures in the same ratios) increases the rate and selectivity for CO insertion and enhances C_{2+} oxygenate synthesis in the F–T reaction (13). Similarly, increasing the pressure improves the activity and selectivity for propionaldehyde formation in the $CO/H_2/C_2H_4$ reaction over Rh, Ni, and Ru catalysts (14, 16, 17). *In situ* infrared spectroscopy studies reveal that the concentration of adsorbed CO does not change significantly with an increase in total pressure on Rh/SiO_2 catalyst (14, 16). No clear relation between the concentration of adsorbed CO and CO insertion activity has been observed.

The objective of this study is to investigate the effect of total pressure on the average residence time of intermediates leading to the formation of propionaldehyde during the $CO/H_2/C_2H_4$ reaction on Rh/SiO_2. An isotopic pulse method combined with *in situ* infrared spectroscopy has been developed to obtain the average residence times and transient responses of isotopically labeled ^{13}CO and [^{13}C]propionaldehyde ($C_2H_5{}^{13}CHO$) while not disturbing

[1] To whom correspondence should be addressed.

0021-9517/95 $6.00

the steady state of the reaction. The intrinsic rate constant and the surface coverage of intermediates can be determined from the transient response with appropriate mechanistic models (18–24). This pulse method will be shown to be equivalent to the isotopic step method commonly used. The results of this study will be used to elucidate the role of total reaction pressure in the CO insertion reaction.

EXPERIMENTAL

Catalyst Preparation and Characterization

A 4 wt% Rh/SiO_2 catalyst was prepared by the incipient wetness impregnation method. An aqueous solution of $RhCl_3 \cdot 3H_2O$ (Alfa Products) was impregnated into a large pore SiO_2 support (Strem Chemicals, surface area of 350 m^2/g). The ratio of the volume of solution to the weight of silica support used in the impregnation step was 1 cm^3 to 1 g. After impregnation, the sample powder was dried in air at 298 K overnight and then reduced under flowing hydrogen at 673 K for 16 h. The H_2 uptake of the catalyst was measured at 303 K by the pulse adsorption method and was found to be 122 μmol/g. This corresponds to a dispersion of 0.62 and a crystallite size of 15 Å, assuming an adsorption stoichiometry of $H_{ads}/Rh = 1$ and a cubic shape of Rh crystallites.

Experimental Apparatus and Procedure

The apparatus used in this study is similar to that previously reported (23) and will be briefly discussed here. Steady-state flows of CO, ^{13}CO, H_2, and C_2H_4 were controlled by mass flow controllers to an infrared (IR) reactor cell. The CO contains 2 vol% Ar for determining the effect of gas-phase holdup in the reactor and the gas transportation lines on the transient response of gaseous products. The CO line upstream from the reactor contains a Valco 6-port pulsing valve and a Valco 4-port switching valve for pulsing an amount of ^{13}CO into the CO flow and totally replacing the CO flow with ^{13}CO flow, respectively. All reactant gases are combined at a mixing point before the IR reactor cell.

The *in situ* infrared spectra were recorded by a Nicolet 5SXC spectrometer with a DTGS detector at a resolution of 4 cm^{-1}. The IR reactor cell, which acts as a differential reactor and has a void volume of 0.64 cm^3, has been described previously (14). The use of a total flow rate of 60 cm^3/min results in a residence time of 0.63 s for the reactant mixture in the IR reactor cell at 0.1 MPa. Thirty-two scans were coadded when recording spectra under steady-state conditions, while only three scans were co-added under transient conditions to facilitate rapid scanning.

The transient responses of the gaseous products from the IR cell were recorded by a Balzers QMG112 mass spectrometer (MS) interfaced to a microcomputer. The MS is equipped with a differentially pumped inlet system located directly downstream of a pressure regulator for fast response time. The *m/e* ratios followed by the MS were 28 for CO, 29 for ^{13}CO, 40 for Ar, and 59 for $C_2H_5{}^{13}CHO$. The *m/e* ratios were carefully selected to prevent interference from the fragmentation of parent species. The concentrations of gaseous products were also analyzed by an HP-5890A gas chromatograph with an FID detector.

Approximately 60 mg of catalyst powder was pressed into a self-supporting disc and placed into the IR reactor cell. The catalyst was further reduced under H_2 flow at 503 K and 0.1 MPa for 2 h prior to the experiments. The reactant gases of $CO/H_2/C_2H_4$ were passed over the catalyst at a 1/1/1 ratio and a total flow rate of 60 cm^3/min. The reaction was allowed to settle to steady state for 20 min before each transient experiment. A pulse of volume 10 cm^3 of ^{13}CO was made into the CO stream, and the pulse transient response of adsorbed CO was recorded by the IR spectrometer and the gaseous products by the MS. It was attempted to keep the pressure within the sampling loop of the 6-port pulsing valve and that of the reactor exactly the same so as to maintain the steady state of the reaction during the pulse injection of ^{13}CO. The pressure was then increased to the next condition and the experiment repeated at the same reactant ratio. The pressure conditions used in this study were 0.1, 0.3, 0.4, and 0.5 MPa. After all experimental runs, the experiment was repeated at 0.1 MPa to determine the reproducibility. Standard deviation for the τ determined from repeated runs is 0.05. A step from CO flow to ^{13}CO flow was also performed at 0.1 MPa to produce a step transient response for comparison with the pulse response under the same conditions.

RESULTS

Steady-State Reaction Measurements

Steady-state reaction rates were measured for hydrocarbon and oxygenated products from the $CO/H_2/C_2H_4$ reaction over 4 wt% Rh/SiO_2 at 503 K and 0.1–0.5 MPa. Table 1 reports the turnover frequencies (TOF) for product formation. The turnover frequency is defined as the rate of product formation (μmol/g-min) divided by the number of surface Rh atoms per gram of catalyst measured by H_2 pulse chemisorption at 303 K. The hydrocarbons in the product consisted of ethane, the product of the hydrogenation of ethylene, and trace amounts of methane, propane, and *n*-butane. The only oxygenated product was propionaldehyde, the product of ethylene hydroformylation.

Increasing the total pressure, while keeping the ratio of the reactants constant, increased the TOF for ethylene

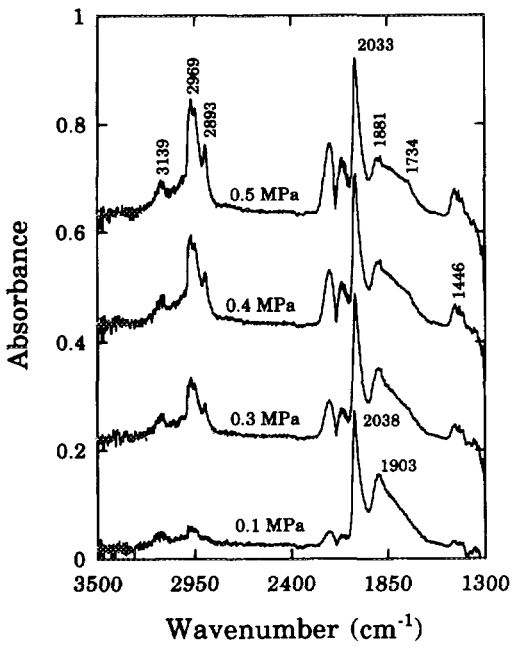

FIG. 1. *In situ* infrared spectra of ethylene hydroformylation over 4 wt% Rh/SiO_2 at 0.1, 0.3, 0.4, and 0.5 MPa.

TABLE 1

The Rate and Selectivity for Product Formation during $CO/H_2/C_2H_4$ Reaction at 503 K $CO/H_2/C_2H_4$ = 1/1/1 on Rh/SiO_2 at 503 K

	Pressure (MPa)			
	0.1	0.3	0.4	0.5
	Turnover frequency ($\times 10^3$) (min^{-1})[a]			
Product:				
CH_4	0.03	0.03	0.02	0.03
C_2H_6	136.2	192.2	181.9	183.0
C_2H_5CHO	20.4	47.8	55.2	60.0
C_3H_6	0.03	0.04	0.04	—
C_4H_8	0.04	0.03	—	0.01
n-C_4H_{10}	0.09	0.02	—	0.03
	Selectivity			
$\frac{TOF_{C_2H_5CHO}}{TOF_{C_2H_6}}$	0.15	0.25	0.30	0.33

[a] H_2 uptake at 298 K = 122 μmol/g.

hydrogenation from 0.1 to 0.3 MPa. Further increasing pressure from 0.3 to 0.4 MPa slightly decreased the TOF for ethylene hydrogenation and caused little change from 0.4 to 0.5 MPa. The TOF for propionaldehyde formation increased with an increase in pressure, as did the selectivity for propionaldehyde formation to that of ethane formation. The selectivity ($TOF_{C_2H_5CHO}/TOF_{C_2H_6}$) is defined as the ratio of the rate of CO insertion into the surface C_2H_x species to the rate of hydrogenation of the C_2H_x species. The rates of these two surface reactions do not exhibit the same total pressure dependence.

Figure 1 depicts the *in situ* IR spectra recorded during the steady-state experiments, the rates of which are reported in Table 1. At 0.1 MPa, the IR spectra feature a linear CO band at 2038 cm^{-1}, a bridged CO band at 1903 cm^{-1}, gaseous ethylene bands at 1446 and 3139 cm^{-1}, a gaseous ethane band at 2969 cm^{-1} (25), and bands at 2947 and 2893 cm^{-1} that may be assigned to the asymmetric and symmetric stretching frequencies of a CH_3 group of surface hydrocarbons, respectively, perhaps ethylidyne, (26, 27). Due to extensive band overlap in the 2800–3100 cm^{-1} region, the relative intensities of the bands at 2947 and 2893 could not be discerned. The intensity of the 2947, 2893, 1446, 3139, and 2969 cm^{-1} bands increased linearly with an increase in pressure from 0.1 to 0.5 MPa and exhibited no change in position. Increasing the pressure from 0.1 to 0.5 MPa increased the intensity of linear CO, excluding the contribution from gaseous CO, by 10% and caused a slight downward shift of linear CO to 2033 and bridged CO to 1881 cm^{-1}. The decrease in the wavenumber of adsorbed CO may be due to a decrease in dipole–dipole interaction resulting from a dilution effect of the increasing surface hydrocarbon concentration (28). The appearance of a shoulder at 1734 cm^{-1} at pressures greater than 0.1 MPa is attributed to propionaldehyde.

In separate experiments, the steady-state reaction rate was measured as a function of temperature in the same IR cell at 0.1 and 0.4 MPa pressure. The results are plotted in Arrhenius form in Fig. 2. The activation energy for

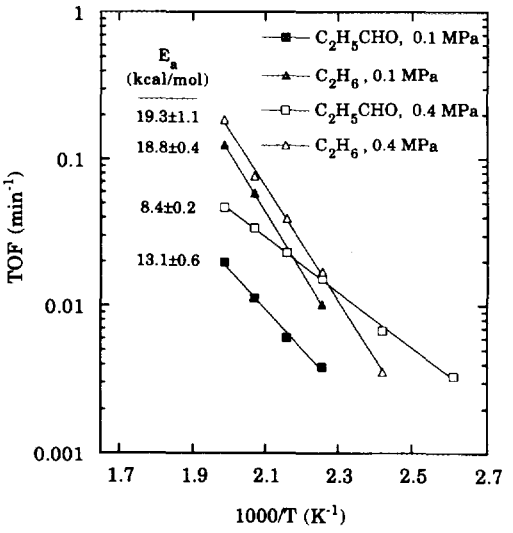

FIG. 2. The effect of temperature on the $CO/H_2/C_2H_4$ reaction at 0.1 and 0.4 MPa ($CO/H_2/C_2H_4$ = 1/1/1).

ethylene hydrogenation remained relatively constant at approximately 19 kcal/mol from 0.1 to 0.4 MPa. The measured activation energy for ethylene hydrogenation is higher than that previously reported for Ni film and supported Pt (29, 30) at a lower temperature range; however, the activation energy agrees well with the results for olefin hydrogenation in propylene hydroformylation on Rh/SiO_2 and zeolite-supported Rh (31, 32). The high activation energy for olefin hydrogenation in the presence of CO may be due to the inhibition of hydrogen and olefin adsorption brought about by adsorbed CO.

The activation energy for propionaldehyde formation decreased from 13.1 to 8.4 kcal/mol with an increase in pressure from 0.1 to 0.4 MPa. The rate of propionaldehyde formation was measured at lower temperatures to test the linearity of the Arrhenius curve at low temperatures. The linearity of the propionaldehyde formation rate over a wide range of temperatures suggests that the low activation energy for propionaldehyde formation is not a result of mass transfer limitations on the reaction rate.

To further confirm the absence of mass transfer limitations, the Weisz–Prater criterion (33, 34) was applied to the results at 503 K and 0.4 MPa. Specifically, the criterion used is

$$\Phi = \frac{(r_{C_2H_5CHO})_{obs}\rho_s L^2}{D_e C_{CO}} \ll 1. \qquad [1]$$

In this equation, ρ_s is the bulk density of the catalyst; L is the thickness of the disk; D_e is the effective diffusivity of CO; and C_{CO} is the concentration of CO at the surface of the pellet. Equation [1] assumes first-order kinetics in CO concentration and is used as an approximation. To obtain the effective diffusivity, the method of Fuller *et al.* (see Ref. 35) was used to estimate the binary diffusivities of CO in C_2H_5CHO, H_2, and C_2H_4 at 0.4 MPa. The smallest value of the binary diffusivity was that of the $CO–C_2H_5CHO$ system at 0.043 cm^2/s. This value was used with tortuosity and porosity of the pellet in the calculation of the Weisz–Prater criterion to obtain an upper limit of $\Phi = 0.0093$. The small value of Φ at 0.4 MPa and the linearity of the Arrhenius curve over a wide range of temperatures suggest that mass transfer is not limiting the rate of propionaldehyde formation and affecting the activation energy. The decrease in the overall activation energy is due to a decrease in the activation energy of the surface reaction steps.

Transient Measurements

To investigate the effect of the total pressure on the intrinsic kinetics and surface coverages of intermediates, isotopic pulse experiments were performed with *in situ* IR spectroscopy. Figure 3 shows the results of a 10 cm^3 pulse of ^{13}CO into the CO/Ar inlet flow at 0.1 MPa and 503 K. Shown in the figure is the transient response of Ar, ^{12}CO, ^{13}CO, and $C_2H_5{}^{13}CHO$. $E(t)$ is the normalized pulse response which is determined from

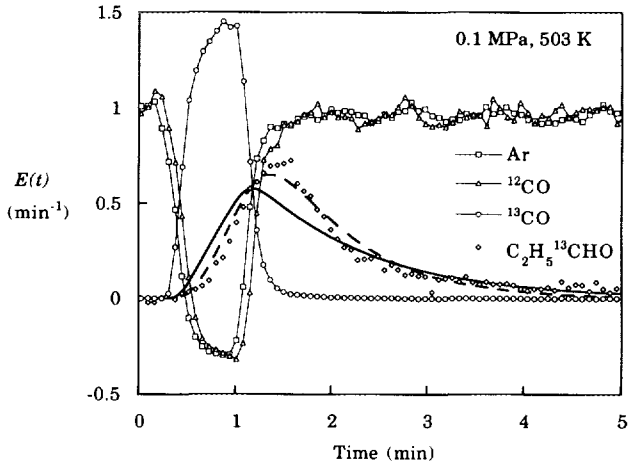

FIG. 3. The transient response of Ar, ^{13}CO, and $C_2H_5{}^{13}CHO$ to a pulse of ^{13}CO in the ^{12}CO feed during ethylene hydroformylation on 4 wt% Rh/SiO_2 at 503 K and 0.1 MPa. The thick solid line for the propionaldehyde response is the one-intermediate pool model response and the dashed line is the two-intermediate pool model response.

$$E(t) = \frac{C(t)}{\int_0^\infty C(t)\,dt}, \qquad [2]$$

where $C(t)$ is the concentration of the tracer species measured by MS. The response is plotted with $E(t) \cdot (P/0.1$ MPa) vs ϕ in Figs. 5–7 for visual comparison of the transient responses at various total pressures. The abscissa, ϕ, is a time scale normalized to 0.1 MPa due to the difference in the gas-phase holdup in the reactor at different total pressures and is determined by

$$\phi = t \cdot \left(\frac{0.1\text{ MPa}}{P}\right), \qquad [3]$$

where t is the time elapsed during the experiment and P is the total pressure. Equations [2] and [3] permit direct comparisons of the transient tracer data at various total pressures.

The symmetrical nature of the ^{12}CO and ^{13}CO responses in Fig. 3 indicates that the species displaced each other and the total concentration of isotopic and nonisotopic CO remained the same during the pulse. The steady state of the surface-catalyzed reaction was maintained during the isotopic pulse transient study. The lag time between the Ar response and the ^{13}CO response is due to interac-

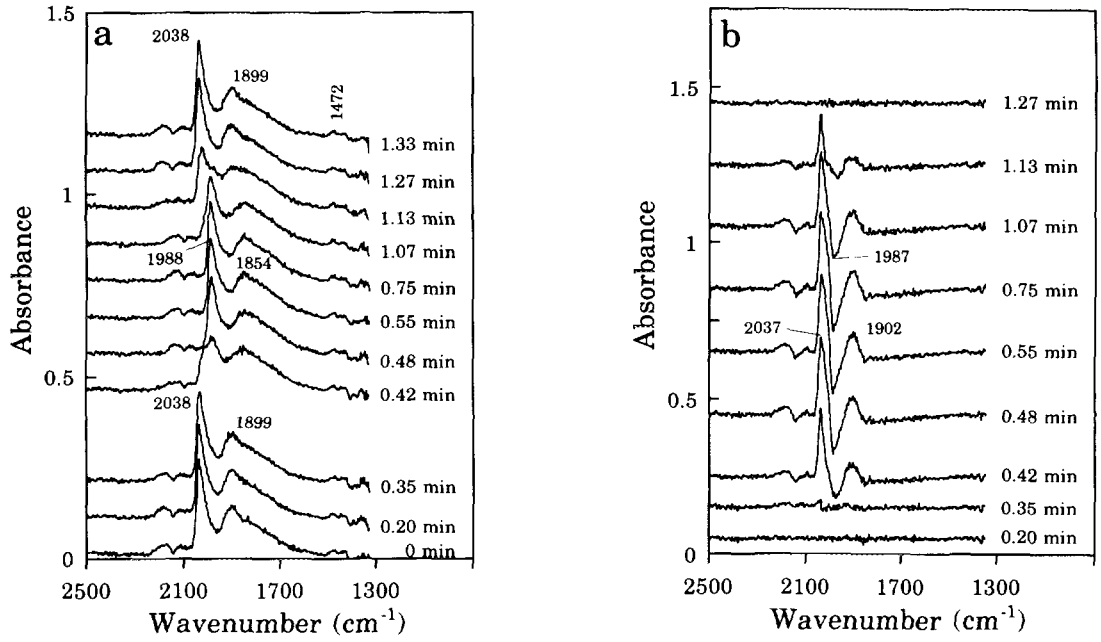

FIG. 4. The transient response of the infrared spectra to a pulse of ^{13}CO in the ^{12}CO feed during ethylene hydroformylation on 4 wt% Rh/SiO_2 at 503 K and 0.1 MPa: (a) the recorded spectra and (b) the difference spectra between the first and each subsequent spectra.

tion of the gas-phase CO with adsorbed CO, i.e., adsorption and desorption. The time delay in the ^{13}C propionaldehyde response as compared to Ar is equivalent to the residence time of ^{13}C surface intermediates leading to propionaldehyde formation. These surface intermediates are derived from ^{13}CO.

Figure 4 shows the IR spectra during the isotopic pulse experiment at 0.1 MPa and 503 K. Figure 4a is the actual spectra recorded and shows that gaseous ^{12}CO is replaced by ^{13}CO in the reactor for approximately 0.75 min, and then returns to the original ^{12}CO flow. The linear and bridged ^{12}CO at 2038 and 1899 cm^{-1}, respectively, also exchange with linear and bridged ^{13}CO at 1988 and 1854 cm^{-1}, respectively, at a very rapid rate. Figure 4b is the spectra recorded at time t and subtracted from that at $t = 0$. This figure shows that the gas phase CO and adsorbed CO exchange with their isotopic counterparts at a rapid rate. Figure 4b also shows that the exchange is complete at $t = 1.27$ min, which is in agreement with the gas-phase ^{13}CO response in Fig. 3. The rates of exchange of linear and bridged CO with either the gas phase or with each other is significantly larger than the scanning rate of our FTIR (0.25 scans/s). The rapid exchange between gaseous and adsorbed CO has also been observed for heterogeneous hydroformylation and CO hydrogenation on Rh/SiO_2 prepared by impregnation with Rh nitrate (23, 36) and Ru/SiO_2 (37). No other feature in the IR spectra changed during the course of the experiment, including those attributed to hydrocarbon surface species and gaseous products.

The results of pulse experiments at 503 K and 0.3, 0.4, and 0.5 MPa are shown in Figs. 5, 6, and 7, respectively. Comparison of isotopic pulse responses in these figures shows that increasing total pressure from 0.1 to 0.4 MPa decreases the residence time for propionaldehyde formation. It is important to note that the Ar response in the pulse experiments at 0.4 MPa and, to a larger extent, at 0.5 MPa exhibit a small hump preceding the actual pulse due to a pressure imbalance between the sample loop containing the isotope tracer and the reactant feed. The regulator on the isotope lecture bottle used in the experiments supplied a maximum downstream pressure of 0.40 MPa. When the pulse was made, the flow of CO to the reactor stopped momentarily until the pressures equilibrated. The Ar response initially decreased when the flow was stopped, then increased when the pressure equilibrated, followed by the displacement with ^{13}CO. Despite the disturbance in the steady-state condition of the reaction, the ^{12}CO and ^{13}CO responses returned to a symmetrical nature rapidly. The oscillating behavior of the Ar response at pressures greater than 0.1 MPa are attributed to the use of a mass flow controller that was originally calibrated for N_2 and contains an oversized orifice.

Figure 8a is the IR spectra response to the isotopic pulse at 0.4 MPa. The IR response of the isotopic pulses at 0.3 and 0.5 MPa yield similar results. The IR spectra response of the pulse experiments at 0.3, 0.4, and 0.5 MPa showed that the linear and bridged adsorbed CO bands exchanged rapidly with the gaseous CO as with the pulse experiment at 0.1 MPa. Not at any time throughout

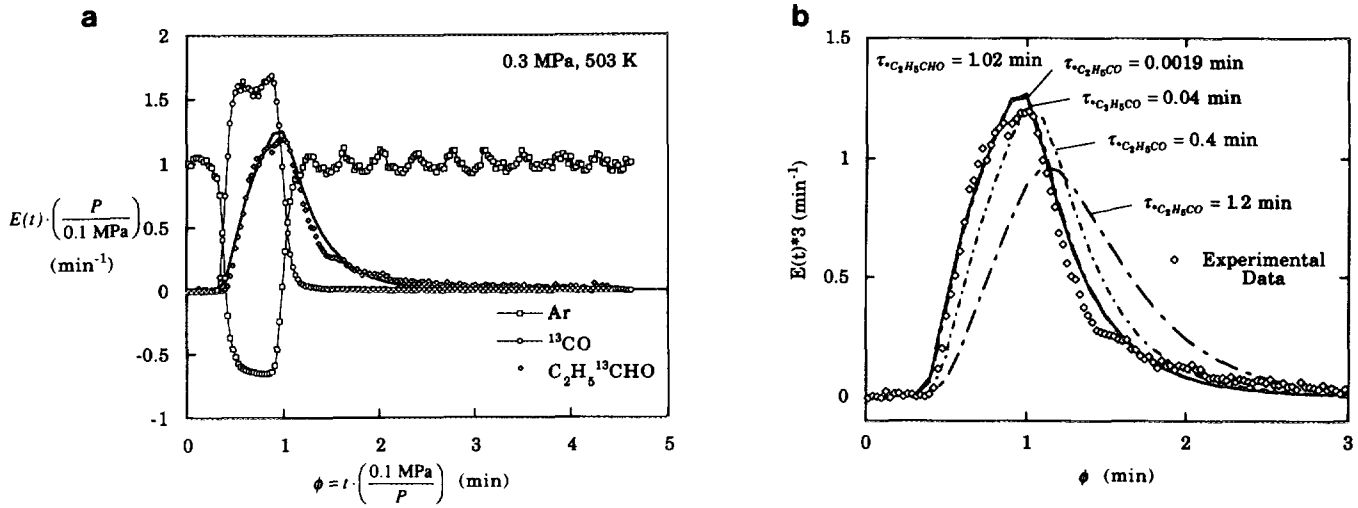

FIG. 5. (a) The transient response of Ar, ^{13}CO, and $C_2H_5{}^{13}CHO$ to a pulse of ^{13}CO in the ^{12}CO feed during ethylene hydroformylation on 4 wt% Rh/SiO_2 at 503 K and 0.3 MPa. (b) The model response of $C_2H_5{}^{13}CHO$ to a pulse of ^{13}CO in the ^{12}CO feed during ethylene hydroformylation on 4 wt% Rh/SiO_2 at 503 K and 0.3 MPa using the two-intermediate pool model.

the transient experiments did the hydrocarbon bands change in wavenumber or intensity. This implies that the hydrocarbons formed in the reaction come mainly from ethylene instead of dissociated CO. The low CH_4 activity for the catalyst in Table 1 further implies that CO dissociation does not occur to a great extent under hydroformylation conditions. The strong bridged CO band made it difficult to discern whether changes occurred in either position or intensity to the shoulder at 1734 cm^{-1}. Figure 8b shows the difference spectra during the isotopic pulse at 0.4 MPa and shows little change in the 1734 cm^{-1} region. This implies that part of the propionaldehyde migrated onto the support surface and did not desorb into the gas phase during the course of the transient study.

The average residence times of each species calculated from the pulse tracer experiments are tabulated in Table 2. The average residence time of the Ar tracer through the reactor system is calculated from

$$\tau_{Ar} = \int_0^\infty t \cdot E_{Ar}(t)\, dt. \qquad [4]$$

Assuming that the flow pattern of gaseous products is the same as that of Ar, the average residence time of surface

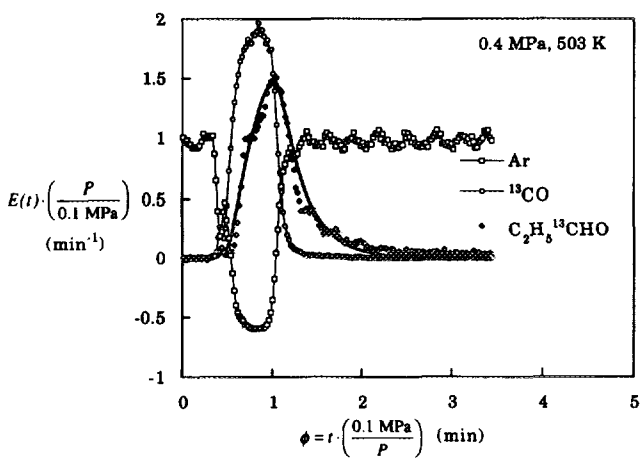

FIG. 6. The transient response of Ar, ^{13}CO, and $C_2H_5{}^{13}CHO$ to a pulse of ^{13}CO in the ^{12}CO feed during ethylene hydroformylation on 4 wt% Rh/SiO_2 at 503 K and 0.4 MPa.

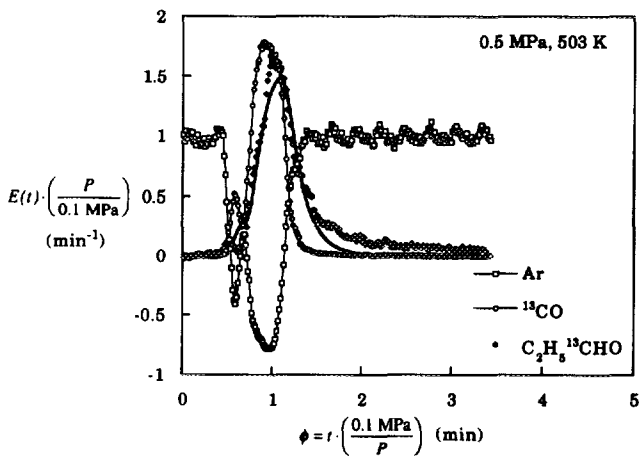

FIG. 7. The transient response of Ar, ^{13}CO, and $C_2H_5{}^{13}CHO$ to a pulse of ^{13}CO in the ^{12}CO feed during ethylene hydroformylation on 4 wt% Rh/SiO_2 at 503 K and 0.5 MPa.

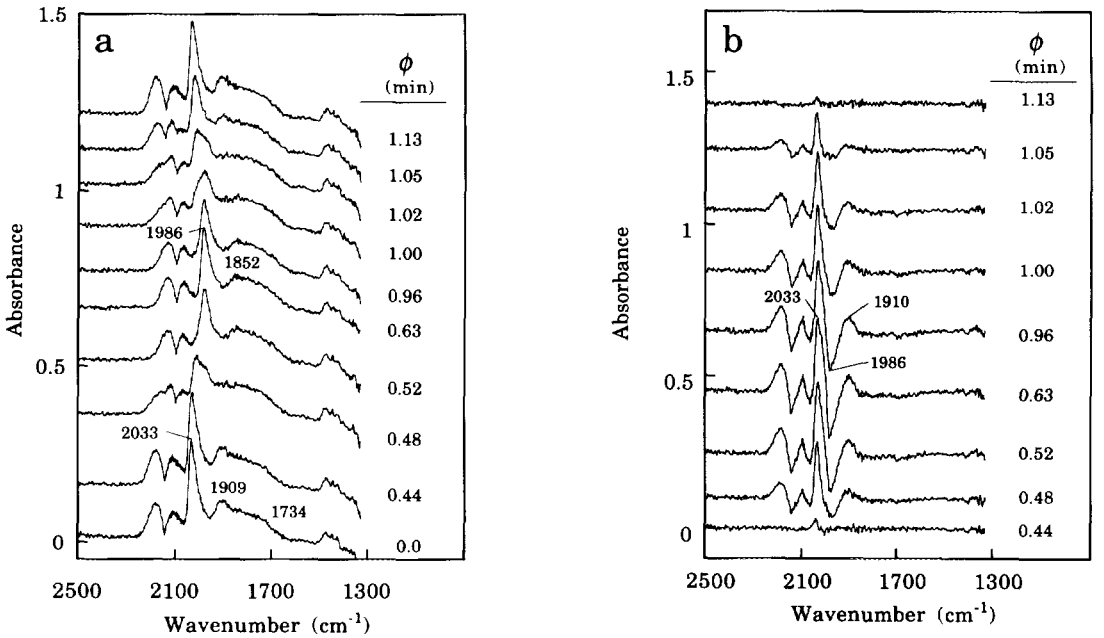

FIG. 8. The transient response of the infrared spectra to a pulse of ^{13}CO in the ^{12}CO feed during ethylene hydroformylation on 4 wt% Rh/SiO_2 at 503 K and 0.4 MPa: (a) the recorded spectra and (b) the difference spectra between the first and each subsequent spectra.

intermediates leading to the gaseous product i is obtained from

$$\tau_i = \int_0^\infty t \cdot E_i(t)\, dt - \tau_{Ar}. \qquad [5]$$

By subtracting the average residence time of the Ar tracer through the reactor system, the average residence time for the product i reflects the residence time of surface intermediates leading to product i.

TABLE 2

The Results of Isotopic Tracer Experiments during $CO/H_2/C_2H_4$ Reaction at 503 K $CO/H_2/C_2H_4$ = 1/1/1 on Rh/SiO_2 at 503 K

Total pressure (MPa)	Average residence time, τ (min)				
	Ar[a]	^{12}CO[b]	^{13}CO[b]	$C_2H_5{}^{13}CHO$[b]	$\theta'_{C_2H_5CHO}$
0.1 (Pulse)	0.73	0.05	0.05	1.31	0.027
0.1 (Switch)	0.70	0.05	0.05	1.40	0.029
0.3	2.1	0.05	0.06	1.11	0.053
0.4	2.9	0.06	0.06	1.00	0.055
0.5	4.0	0.08	0.20	1.16[c]	0.069[c]

[a] Calculated from Eq. [4].
[b] Calculated from Eq. [5].
[c] This value is an upper limit due to the imbalance in pressure between the reactor and the sample loop (see text).

In Table 2, the residence times of the Ar response are similar within experimental error when multiplied by the normalization factor, (0.1 MPa/P), due to an increase in total pressure. By maintaining the steady-state conditions, the average residence times of ^{12}CO and ^{13}CO were equal for all but the pulse tracer experiment at 0.5 MPa. As pointed out qualitatively in Figs. 3 and 4, the residence times for propionaldehyde formation decreased with an increase in pressure. Due to the inequality of the pressure between the sample loop and reactor, the first peak of the Ar response at 0.5 MPa causes an overestimate of τ_{Ar} so that it does not reflect the gas flow pattern that carries the ^{13}CO and ^{13}C propionaldehyde response. Due to the overestimate of τ_{Ar}, the calculated average residence time of propionaldehyde formation for 0.5 MPa should be considered as an upper limit.

A pulse study was performed to determine the contribution of physisorption on the average residence time of the propionaldehyde species. Pulses of propionaldehyde in inert He flow were conducted through the reactor bypass and through the reactor with a catalyst disc at 503 K and at both 0.1 and 0.4 MPa. Figure 9 shows that the pulses through the reactor exhibited a delay in the response of propionaldehyde due to the gas-phase hold up in the reactor. This result shows that physisorption and readsorption of the propionaldehyde product do not play a significant role in the average residence times (τ) for the formation of gaseous propionaldehyde. The extent of readsorption depends on the ratio of adsorption rate to carrier gas flow

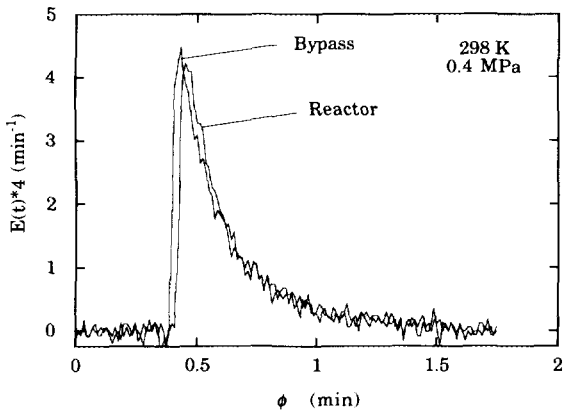

FIG. 9. A pulse of propionaldehyde at 0.4 MPa and 503 K through the reactor bypass and through the reactor.

rate (38), the amount of catalyst, and reactor configuration. Low ratio of adsorption rate to carrier gas ($\ll 1$) and the use of thin catalyst disc minimize the readsorption.

Most transient isotopic studies involve the use of a step switch from a reactant to an isotopically labeled reactant (18–24). Few pulse isotopic transient studies have been used to elucidate the reaction pathway for CO hydrogenation and partial oxidation of CH_4 (39, 40).

For steady-state flow systems, both pulse and step responses should produce the same information. According to the theory of residence time distributions, the response of the pulse tracer input is quantitatively equivalent to the derivative of the response of a step tracer input with respect to time (41). One potential inconvenience of the pulse technique is the selection of a proper amount of tracer which could stay in the reactor long enough to be incorporated into a reaction pathway so that the labeled product can be detected in the effluent with reasonable accuracy. Peil *et al.* suggested that a step input be used for a reaction which consists of more than one pathway (42). A step input allows the response of the labeled species produced from all intermediate pools with various reactivities to reach steady state. However, the high cost of isotope reactants does not often allow the use of step inputs to study catalytic reactions at high pressure. The problem of a low reactive intermediate pool can be overcome by the use of a larger amount of tracer in the pulse experiment.

Three main factors affecting the accuracy of the response measurement of a tracer product in a pulse experiment are the size of the pulse, the average residence time of the intermediate pools (intrinsic kinetics), and the sensitivity of the detecting device. As the amount of pulsed tracer increases, the probability of the tracer to be incorporated into the reaction pathway increases and the initial response approaches the response of a step input. Highly reactive intermediates (with small residence times) will incorporate more tracer species into the pathway than those with lower reactive intermediates (having large residence times). The quality of the transient information, i.e., the signal-to-noise ratio of the response, is governed by the scanning rate and the sensitivity of the detecting device. These factors must be considered in the design of pulse tracer experiments.

To verify whether all the transient information is obtained from the pulse tracer experiments for the $CO/H_2/C_2H_4$ reaction, a step tracer experiment from CO to ^{13}CO was conducted at 0.1 MPa. The resulting gas-phase response is presented in Fig. 10. The step response is normalized according to

$$F(t) = \frac{C(t) - C^0}{C^\infty - C^0}, \qquad [6]$$

where $F(t)$ is the normalized response function and C^∞ and C^0 are the concentration of tracer species at $t = 0$ and $t = \infty$, respectively. If the input pulse shown in Fig. 3 can be approximated by an impulse function, the relation

$$F(t) = \int_0^t E(t)\,dt \qquad [7]$$

holds true (41). The symbols in Fig. 10 are the experimental results of the step change in concentration of CO to ^{13}CO and the solid lines are the integration of the points of the pulse with respect to time in Fig. 3. Figure 10 shows that, although the initial pulse is not an impulse, the results from the two experiments agree remarkably well. It should be noted that the step response (the data point in Fig. 10) and integration of the pulse response (the solid line) of Ar with respect to time are not in close agreement

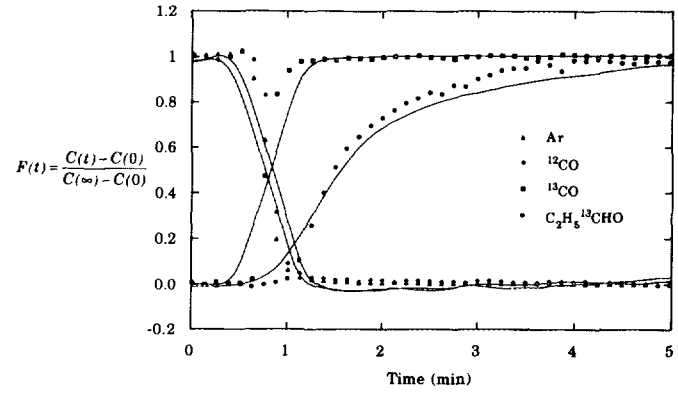

FIG. 10. Comparison of a step change of $^{12}CO/H_2/C_2H_4$ to $^{13}CO/H_2/C_2H_4$ over 4 wt% Rh/SiO_2 catalyst at 503 K and 0.1 MPa. The lines are the result of integration of a pulse response of ^{13}CO in ^{12}CO under the same conditions.

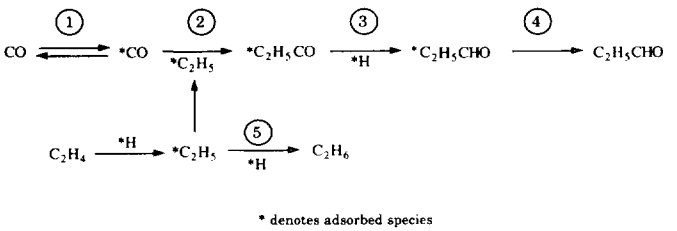

FIG. 11. The reaction scheme for the formation of ethane and propionaldehyde from $CO/H_2/C_2H_4$ on Rh/SiO_2.

as compared with the responses of propionaldehyde. This is because both pulse and step injections deviated from their perfect modes to a different extent. Such a difference in the input to the system is alleviated by the slow responses of propionaldehyde. The slow response of propionaldehyde also allows the input pulse to be approximated by an impulse function. The average residence time determined from a transient experiment should be independent of the input function if the steady-state conditions were maintained during the transient study. The residence times of propionaldehyde determined from both step and pulse inputs shown in Table 2 are consistent within experimental error. These results suggest that the pulse tracer experiments capture the transient nature of the propionaldehyde response for $CO/H_2/C_2H_4$ system on Rh/SiO_2 and the pulse tracer method is a more economical approach to use costly isotope under high pressure conditions.

DISCUSSION

Mechanistic and kinetic information on the reactivity of intermediates can be derived from a postulated mechanistic model with mathematical analysis of the transient response. The mechanism for heterogeneous hydroformylation has been postulated from analogy with the homogeneous hydroformylation reaction (2, 4, 14). The generally accepted mechanism of the reaction is shown in Fig. 11. The formation of propionaldehyde involves the partial hydrogenation of C_2H_4 to form an adsorbed ethyl species, insertion of adsorbed linear CO into the adsorbed ethyl species to form an adsorbed acyl species, and hydrogenation of the acyl species to produce propionaldehyde. Hydrogenation of the adsorbed ethyl species results in the formation of ethane. The same type of surface adsorbed hydrogen is assumed to hydrogenate both the acyl and ethyl intermediates. The rates of chain growth and methanation are too small to be considered in the present study.

The proposed reaction scheme in Fig. 11 suggests that the adsorbed ethyl species may undergo either hydrogenation or CO insertion; hydrogenation is a competing reaction with the CO insertion step. Mechanistic studies of homogeneous hydroformylation and hydrogenation have shown that an alkyl ligand on a mononuclear $Rh(CH_2CH_2R)(CO)(PPh_3)_2$ complex can undergo either hydrogenation or CO insertion depending on the addition of either a hydrogen atom or another CO ligand to the Rh metal center (43). Based on analogy between homogeneous and heterogeneous hydroformylation and substantiating kinetic data for propylene and ethylene hydroformylation (14, 31, 44, 45), we speculate that the $*C_2H_5$ surface species is an intermediate for both ethane and propionaldehyde production. The probability of the surface ethyl species to undergo either hydrogenation or CO insertion may depend on the neighboring adsorbed species and sites.

The observed D_2 isotope effect on butyraldehyde formation and analysis of kinetic data suggest the hydrogenation of the acyl species is the rate-determining step for butyraldehyde formation on Rh/SiO_2 and $Rh–Co/SiO_2$ catalysts at a total pressure of 20–70 kPa and 50–70 kPa, respectively (31, 44, 45). The observed decrease in the overall activation energy for propionaldehyde with increasing total pressure suggests that total pressure has a great impact on the rate constants of elementary steps and may change the rate-determining step. Under steady-state reaction condition, the rate of propionaldehyde formation can be described by

$$TOF_{C_2H_5CHO} = k_3\theta_{*H}\theta_{*C_2H_5CHO} = k_4\theta_{*C_2H_5CHO}, \quad [8]$$

while the rate of ethane formation can be represented by

$$TOF_{C_2H_6} = k_5\theta_{*H}\theta_{*C_2H_5}. \quad [9]$$

Examination of Eqs. [8] and [9] shows that both $TOF_{C_2H_5CHO}$ and $TOF_{C_2H_6}$ are proportional to θ_{*H}, suggesting that the observed increase in selectivity and TOF for propionaldehyde formation with an increase in pressure is not due to an increase in adsorbed molecular hydrogen coverage. The increase in selectivity and TOF for propionaldehyde may be related to the effect of total pressure on kinetic parameters (i.e., k_3, k_4, and k_5), $\theta_{*C_2H_5O}$, and $\theta_{*C_2H_5CHO}$.

The acyl species or the chemisorbed propionaldehyde in the mechanism shown in Fig. 11 cannot be directly observed by the IR spectra because their concentrations on the catalyst surface are low and their infrared bands are overlapped with the broad bridged CO band under the conditions of this study. Without direct observation of the acyl intermediate, the surface coverage may be inferred from mathematical analysis of the transient response. A number of analyses can be applied to the transient responses depending on the postulated mechanism.

The most basic analysis assumes a single intermediate pool and one irreversible reaction pathway from reaction

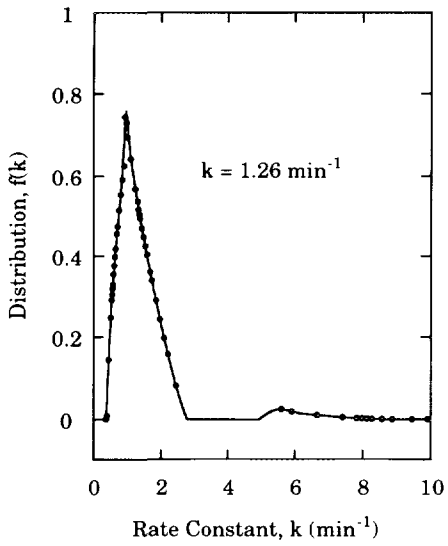

FIG. 12. The rate constant distribution of propionaldehyde formation from $CO/H_2/C_2H_4$ on 4 wt% Rh/SiO_2 at 503 K and 0.1 MPa calculated from steady-state isotopic data.

intermediate to product. Biloen *et al.* (46) showed that for an irreversible surface reaction step with a single intermediate surface pool, the surface coverage of intermediates leading to a product i can be calculated from

$$\theta_i = \mathrm{TOF}_i \cdot \tau_i, \qquad [10]$$

where θ_i is defined as the surface coverage of all intermediate species that will eventually be incorporated into product i. Table 2 reports the values of θ_i for $i = C_2H_5CHO$ determined from Eq. [10]. The surface coverage, $\theta'_{C_2H_5CHO}$, increased with an increase in total reaction pressure from 0.1 to 0.4 MPa. It must be noted that the surface coverage is an upper limit for the 0.5 MPa case due to the imbalance in pressure discussed previously. From this analysis, it is evident that the surface coverages of all the adsorbed intermediates, i.e., the acyl species and chemisorbed propionaldehyde, increase with an increase in pressure from 0.1 to 0.5 MPa.

It is logical to extend the previous assumption of a single intermediate pool to numerous intermediate pools in parallel, i.e., a heterogeneous surface exhibiting a broad spectrum of reactivities. The results of the step transient response permit the elucidation of the extent of surface heterogeneity for the formation of propionaldehyde. De Pontes *et al.* (47) and Hoost and Goodwin (48) developed methods for numerically calculating the rate constant distribution on heterogeneous surfaces using results from isotopic step transient data. These methods are derived from the assumption that the reaction takes place on an infinite number of single intermediate pools in parallel. Figure 12 shows the results of applying the method of de Pontes *et al.* (47) to the step transient of Fig. 10. An initial dead time of 0.6 min after the argon response was observed in the propionaldehyde response. As a result, the analysis was conducted by subtracting 0.6 min from the time scale. The main feature of Fig. 12 is a sharp distribution with a mean value of 1.26 min^{-1}. This result agrees with the average residence time reported in Table 2 for a total pressure of 0.1 MPa when the inverse of 1.26 min^{-1} is added to 0.6 min. The small distribution at higher values of the rate constant is insignificant compared to the larger distribution and can be attributed to noise in the data. This result implies that the formation of propionaldehyde from the $CO/H_2/C_2H_4$ reaction on Rh/SiO_2 occurs mainly from one reaction pathway with a narrow rate constant distribution.

Using isotopic transient data for acetaldehyde formation from syngas, Koerts and van Santen (20) found that acetaldehyde formation occurs with a bimodal distribution of reactivities on Rh/SiO_2 and $V–Rh/SiO_2$. They speculated that a bimodal distribution is a result of a more reactive aldehyde species on the metal surface and a less reactive aldehyde species on the support near the Rh particles. The bimodal distribution of active sites observed by Koerts and van Santen (20) may alternatively be explained by the fact that acetaldehyde from syngas is formed from CO insertion into a CH_x species formed from CO dissociation and partial hydrogenation. The CH_x species formed on Group VIII metal catalysts exhibit a bimodal distribution in activity for hydrogenation to methane on Rh, Ru, and Ni (47–49). It is reasonable to speculate that the surface CH_x species may also exhibit a bimodal rate constant distribution for CO insertion.

Comparison of the available literature on the rate constant distribution for CO related reactions reveals that methanation and the formation of C_2 oxygenates from CO/H_2 exhibit a bimodal rate constant distribution on Ni, Ru, and Rh (20, 21, 47–49). The reaction on these catalysts is classified as a structure-sensitive reaction which takes place on ensemble sites. Interestingly, the formation of propionaldehyde from CO insertion shows entirely different characteristics from methanation. The propionaldehyde formation exhibits a narrow rate constant distribution; the reaction is less structure-sensitive than methanation (50) and takes place on single Rh sites that chemisorb linear CO (14). The direct evidence for propionaldehyde formation on the single Rh site is the simultaneous consumption of linear CO and the formation of propionaldehyde during exposure of adsorbed CO to C_2H_6 and H_2 at 301 K (14). The observed decrease in the wavenumber and intensity of linear CO during the reaction of linear CO (14) suggests the presence of dipole–dipole interactions between neighboring linear CO. These neighboring linear CO species indicate their adsorption sites, i.e., sites for the CO insertion, are not in the isolated state. Further study is required to determine the effect of

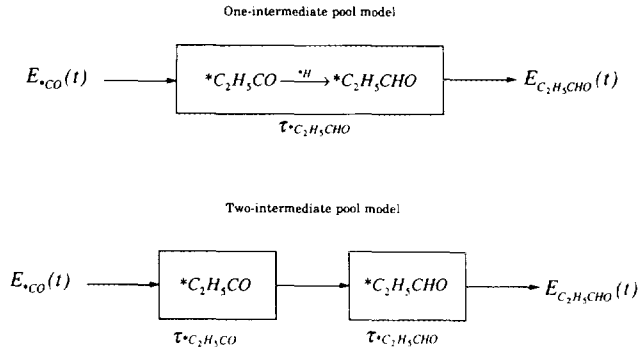

FIG. 13. Schematic of the one-intermediate and two-intermediate pool models.

interactions between neighboring adsorbates and sites on the structure sensitivity of the reaction.

Transient response methods can be used to test various proposed mechanisms in catalytic reactions by modeling the response. The postulation of a single intermediate pool was tested by comparing the model response with the experimental response. The schematic of the one-intermediate pool model, shown in Fig. 13, assumes that the formation of propionaldehyde from a single intermediate pool is an irreversible step. Both adsorbed acyl and adsorbed propionaldehyde are lumped into a single intermediate pool. $E_{*CO}(t)$ and $E_{C_2H_5CHO}(t)$ are the responses of $*^{13}CO$ and $C_2H_5{}^{13}CHO$, respectively, and $\tau_{*C_2H_5CHO}$ is the time constant (the average residence time) of the intermediate in the single pool. The mathematical form of the model is derived from a mole balance of intermediates:

$$\tau_{*C_2H_5CHO}\frac{dE_{C_2H_5CHO}(t)}{dt} = E_{*CO}(t) - E_{C_2H_5CHO}(t). \quad [11]$$

The response of gaseous CO observed by the MS and the response of adsorbed CO observed by the IR coincide so that the gaseous CO response is used as the input function. Since the gas flow has the same effect on $E_{CO}(t)$ and $E_{C_2H_5CHO}(t)$, the effect of the flow pattern on $E_{C_2H_5CHO}(t)$ should not be included in the calculation. Equation [11] was numerically integrated and the parameter $\tau_{*C_2H_5CHO}$ was found by a nonlinear least-squares fit of the propionaldehyde response using the TUTSIM dynamic simulation software package (51). The values of the parameter $\tau_{*C_2H_5CHO}$ found from the data fit for each pressure are shown in Table 3. The quality of the model can be observed from the model response, which is shown as the thick solid lines for the propionaldehyde response in Figs. 3, 5–7. The average residence times reported in Table 3 agree well with those reported in Table 2 for pressures of 0.3–0.5 MPa. The good agreement is due to the use of the same assumptions in obtaining τ in Table 2. This result indicates that all intermediates can be lumped into one intermediate pool in the reaction pathway from adsorbed *CO to gaseous propionaldehyde at pressures greater than 0.1 MPa.

Equation [11] did not fit the data for 0.1 MPa well. To further analyze the results at 0.1 MPa, the adsorbed acyl and adsorbed propionaldehyde are modeled as two intermediate pools in series. The two intermediate pool model, shown in Fig. 13, assumes that the reaction pathway from *CO to gaseous propionaldehyde contains three irreversible steps and two intermediates. The mole balance for the intermediates in this model is

$$\tau_{*C_2H_5CO}\frac{dE_{*C_2H_5CO}(t)}{dt} = E_{*CO}(t) - E_{*C_2H_5CO}(t) \quad [12]$$

$$\tau_{*C_2H_5CHO}\frac{dE_{C_2H_5CHO}(t)}{dt} = E_{*C_2H_5CO}(t) - E_{C_2H_5CHO}(t), \quad [13]$$

where $\tau_{*C_2H_5CO}$ and $\tau_{*C_2H_5CHO}$ are the residence time of the two intermediate species corresponding to the hydrogenation and the desorption steps. The parameters $\tau_{*C_2H_5CO}$ and $\tau_{*C_2H_5CHO}$ were found by numerically fitting Eqs. [12] and [13].

The two-intermediate pool model fits the data well for the propionaldehyde response for 0.1 MPa and the model response is shown by the thick dashed line in Fig. 3. The parameters $\tau_{*C_2H_5CO}$ and $\tau_{*C_2H_5CHO}$ found from the model equations are shown in Table 3 for 0.1 MPa. The good fit of the data suggests that the formation of propionaldehyde from adsorbed *CO involves two intermediates at 0.1 MPa. Values for the model response for $\tau_{*C_2H_5CO}$ and $\tau_{*C_2H_5CHO}$ are interchangeable; assignment of the large or small value to either $\tau_{*C_2H_5CO}$ or $\tau_{*C_2H_5CHO}$ yields the same response. The small residence time at high perssure is assigned to $\tau_{*C_2H_5CO}$. Justification for this assignment will be discussed later.

Table 3 shows that an increase in total reaction pressure significantly decreases one of the residence time values. At total pressures of 0.3 MPa and greater, the residence time of one of the intermediate pools is two orders of magnitude greater than the other one. Figure 5b shows the model response is essentially independent of the small value when it is less than 0.0019 min with an integration step size of 0.001 min at 0.3 MPa. In the two-intermediate pool model, the steady-state reaction rate for propionaldehyde formation can be described by

$$\mathrm{TOF}_{C_2H_5CHO} = k_3'\theta_{*C_2H_5CO} = k_4\theta_{*C_2H_5CHO}, \quad [14]$$

where the rate constant k_3' is $k_3\theta_{*H}$. Equation [14] shows the relationship between the steady-state TOF and the surface coverages and the rate constants are the inverse

TABLE 3

The Results of Fitting the Pulse Tracer Responses to Model Equations

Pressure (MPa)	One-intermediate pool model			Two-intermediate pool model					
	$\tau_{*C_2H_5CHO}$ (min)	k_4 (min^{-1})	θ	$\tau_{*C_2H_5CO}$ (min)	k_3' (min^{-1})	$\theta_{*C_2H_5CO}$	$\tau_{*C_2H_5CHO}$ (min)	k_4 (min^{-1})	$\theta_{*C_2H_5CHO}$
0.1	1.18	0.85	0.024	0.32	3.13	0.007	0.94	1.06	0.019
0.3	1.02	0.98	0.048	<0.0019[a]	>526	$<9.1 \times 10^{-5}$	1.02	0.98	0.049
0.4	0.91	1.09	0.050	<0.0038	>357	$<21 \times 10^{-5}$	0.91	1.10	0.050
0.5	1.08	0.92	0.064	<0.0036	>277	$<22 \times 10^{-5}$	1.08	0.93	0.065

[a] Δh (Integration step size) = 0.001 min.

of the average residence time for each species. The step with a very large rate constant (or the intermediate with a very small residence time) has little impact on the model response and appears to be kinetically insignificant. Therefore, the two-step process can be modeled as a one-step process if one of the rate constants is significantly greater than the other.

The coverage of adsorbed $*C_2H_5CO$ and $*C_2H_5CHO$ can be obtained from Eq. [14] with the measured TOF and rate constants. The two-intermediate pool model in Table 3 shows increasing the total pressure decreases the coverage of adsorbed $*C_2H_5CO$, but increases the coverage ($\theta_{*C_2H_5CHO}$) of adsorbed $*C_2H_5CHO$. The increase in $\theta_{*C_2H_5CHO}$ with total pressure is consistent with the observed increase in the IR intensity of adsorbed propionaldehyde shown in Fig. 1. The consistency in the increasing trend of $\theta_{*C_2H_5CHO}$ obtained from two different approaches justifies the assignment of the small residence time to $\tau_{*C_2H_5CO}$. It should be noted that the sum of $\theta_{*C_2H_5CO}$ and $\theta_{*C_2H_5CHO}$ in Table 3 approximately equals $\theta'_{C_2H_5CHO}$ listed in Table 2, suggesting that Eq. [10] can provide a quick estimate of the coverage of all intermediates leading to gaseous product.

At 0.1 MPa the rate constants k_3' and k_4 are the same order of magnitude, while at higher pressures k_3' is much greater than k_4. The substantial increase in k_3' may be related to the decrease in the overall (apparent) activation energy for propionaldehyde formation from 13.1 to 8.4 kcal/mol with an increase in pressure from 0.1 to 0.4 MPa. An apparent activation energy of 8.4 kcal/mol for the propionaldehyde formation is a good agreement with the heat of desorption of propionaldehyde from the Rh (111) surface obtained from TPD data (52). These results further support that the formation of propionaldehyde is governed by the step involving k_4, the desorption of adsorbed propionaldehyde at high pressure.

Neglecting the compensation effect and the heat of desorption of adsorbed propionaldehyde, a decrease in the overall activation energy for a reaction of 4.7 kcal/mol reflects an increase in the rate constant by a factor of 110. This agrees well with a more than 114-fold increase in k_3' from 0.1 to 0.4 MPa reported in Table 3. The cause of the increase in k_3' with increasing pressure remains to be investigated.

CONCLUSIONS

The results of pulse and step isotopic transient study show that the pulse method produced the same mechanistic information as the commonly used step method. The pulse method permits the use of low quantities of costly isotope to study reactions under high pressure conditions. Steady-state rate measurements reveal that an increase in pressure increases the rate and selectivity of propionaldehyde to ethane and decreases the activation energy of propionaldehyde formation during the $CO/H_2/C_2H_4$ reaction on Rh/SiO_2. Analysis of the isotopic pulse response shows that an increase in pressure from 0.1 to 0.5 MPa increases the coverage of intermediates, but decreases the average residence time. Modeling of the transient responses reveals that the formation of propionaldehyde from adsorbed CO involves three irreversible steps and two intermediates, perhaps adsorbed acyl and adsorbed propionaldehyde. Increasing the pressure causes a significant increase in the rate of hydrogenation of adsorbed acyl which may be related to the decrease in the overall activation energy of propionaldehyde formation. Rate constant analysis of the propionaldehyde response shows that the rate constant for propionaldehyde formation exhibits a sharp single distribution.

ACKNOWLEDGMENT

M.W.B. gratefully acknowledges financial support from the Department of Chemical Engineering at the University of Akron.

REFERENCES

1. Chuang, S. C., Goodwin, J. G., Jr., and Wender, I., *J. Catal.* **92,** 416 (1985).

2. Chuang, S. C., Tian, Y. H., Goodwin, J. G., Jr., and Wender, I., *J. Catal.* **96,** 449 (1985).
3. Pijolat, M., and Perrichon, V., *Appl. Catal.* **13,** 321 (1985).
4. Sachtler, W. M. H., and Ichikawa, M., *J. Phys. Chem.* **90,** 4752 (1986).
5. Jordan, D. S., and Bell, A. T., *J. Phys. Chem.* **90,** 4797 (1986).
6. Gysling, H. J., Monnier, J. R., and Apai, G., *J. Catal.* **103,** 407 (1987).
7. Watson, P. R., and Somorjai, G. A., *J. Catal.* **72,** 347 (1981).
8. Chuang, S. S. C., Pien, S. I., and Narayanan, R., *Appl. Catal.* **57,** 241 (1990).
9. Lou, H. Y., Bastein, A. G. T. M., Mulder, A. A. J. P., and Ponec, V., *Appl. Catal.* **38,** 241 (1988).
10. Chuang, S. S. C., and Pien, S. I., *J. Catal.* **128,** 596 (1991).
11. Orita, H., Shuichi, N., and Tamaru, K., *J. Catal.* **90,** 183 (1984).
12. Underwood, R. P., and Bell, A. T., *J. Catal.* **111,** 325 (1988).
13. Chuang, S. C., Goodwin, J. G., Jr., and Wender, I., *J. Catal.* **95,** 435 (1985).
14. Chuang, S. S. C., and Pien, S. I., *J. Catal.* **135,** 618 (1992).
15. Hinderman, J. P., Huthings, G. J., and Kiennemann, A., *Catal. Rev. Sci. Eng.* **53**(1), 1 (1993).
16. Chuang, S. S. C., and Pien, S. I., *J. Mol. Catal.* **55,** 12 (1989).
17. Chuang, S. S. C., and Pien, S. I., *Catal. Lett.* **3,** 323 (1989).
18. Tamaru, K., *in* "Catalysis: Science and Technology" (J. R. Anderson and M. Boudart, Eds.) Vol. 9, p. 87. Springer-Verlag, Berlin/Hiedelberg/New York, 1991.
19. Stockwell, D. M., Chung, J. S., and Bennett, C. O., *J. Catal.* **112,** 135 (1988).
20. Koerts, T., and van Santen, R. A., *J. Catal.* **134,** 13 (1992).
21. Hoost, T. E., and Goodwin, J. G., Jr., *J. Catal.* **137,** 22 (1992).
22. Krishna, K. R., and Bell, A. T., *J. Catal.* **139,** 104 (1993).
23. Srinivas, G., Chuang, S. S. C., and Balakos, M. W., *AIChE J.* **39,** 530 (1993).
24. Happel, J., "Isotopic Assessment of Heterogeneous Catalysis." Academic Press, New York, 1986.
25. Hair, M. L., "Infrared Spectroscopy in Surface Chemistry." Dekker, New York, 1967.
26. Beebe, T. P., Jr., and Yates, J. T., *J. Phys. Chem.* **91,** 254 (1987).
27. Lapinsky, M. P., and Ekerdt, J. G., *J. Phys. Chem.* **94,** 4599 (1990).
28. Stoop, F., Toolenaar, F. J. C. M., and Ponec, V., *J. Catal.* **73,** 50 (1982).
29. Somorjai, G., "Chemistry in Two Dimensions," p. 445. Cornell Univ. Press, Ithaca/London, 1981.
30. Cortright, R. D., Goddard, S. A., Rekoske, J. E., and Dumesic, J. A., *J. Catal.* **127,** 342 (1991).
31. Naito, S., and Tanimoto, M., *J. Catal.* **130,** 106 (1991).
32. Davis, M. E., Rode, E., Taylor, D., and Hanson, B. E., *J. Catal.* **86,** 67 (1984).
33. Weisz, P. B., and Prater, C. D., *Adv. Catal.* **6,** 143 (1954).
34. Froment, G. F., and Bischoff, K. B., "Chemical Reactor Analysis and Design," p. 167. Wiley, New York, 1990.
35. Reid, R. C., Prausnitz, J. M., and Poling, B. E., "The Properties of Gases and Liquids," p. 587. McGraw–Hill, New York, 1987.
36. Balakos, M. W., Chuang, S. S. C., and Srinivas, G., *J. Catal.* **140,** 281 (1993).
37. Winslow, P., and Bell, A. T., *J. Catal.* **86,** 158 (1984).
38. Demmin, R. A., and Gorte, R. J., *J. Catal.* **90,** 32 (1984).
39. Ekstrom, A., and Lapszewicz, J. A., *J. Phys. Chem.* **93,** 5230 (1989).
40. Siddall, J. H., Miller, M. L., and Delgass, W. N., *Chem. Eng. Commun.* **83,** 261 (1989).
41. Levenspiel, O., "Chemical Reaction Engineering," p. 258. Wiley, New York, 1972.
42. Peil, K. P., Goodwin, J. G., Jr., and Marcelin, G., *J. Phys. Chem.* **93,** 5977 (1989).
43. Cotton, F. A., and Wilkenson, G., "Advanced Inorganic Chemistry," Wiley, New York, 1988.
44. Reut, S. I., Kamalov, G. L., and Golodets, G. I., *React. Kinet. Catal. Lett.* **44**(1), 191 (1991).
45. Reut, S. I., Kamalov, G. L., and Golodets, G. I., *Kinet. Catal. Engl. Transl.* 694 (1991).
46. Biloen, P., Helle, J. N., van den Berg, F. G. A., and Sachtler, W. M. H., *J. Catal.* **81,** 450 (1983).
47. de Pontes, M., Yokomizo, G. H., and Bell, A. T., *J. Catal.* **104,** 147 (1987).
48. Hoost, T. E., and Goodwin, J. G., Jr., *J. Catal.* **134,** 678 (1992).
49. Balakos, M. W., Ph.D. Dissertation, the University of Akron, Akron, OHIO (1994).
50. Chuang, S. S. C., Pien, S. I., and Narayanan, R., *Appl. Catal.* **57,** 241 (1990).
51. Reynolds, W. E., and Wolf, J., "TUTSIM Block Diagram Simulation Language." TUTSIM Products, Palo Alto, CA, 1991.
52. Brown, N. F., and Barteau, M. A., *Langmuir* **8,** 862 (1992).